

January, 1995

# Thermal Properties of a Hot Pion Gas beyond the Quasiparticle Approximation

R. Rapp<sup>1</sup> and J. Wambach<sup>1, 2</sup>

*Department of Physics  
University of Illinois at Urbana-Champaign  
1110 West Green St., Urbana, IL 61801-3080, USA*

## Abstract

Within the Matsubara formalism we derive expressions for the pion selfenergy and the two-pion propagator in a hot pion gas. These quantities are used to selfconsistently calculate the in-medium  $\pi\pi$  amplitude beyond the quasiparticle approximation (QPA). The results are shown to differ significantly from QPA-based calculations. We also examine the impact of chiral constraints on the  $\pi\pi$  interaction in a chirally improved version of the Jülich  $\pi\pi$  model.

PACS Indices: 13.75.Lb  
13.85.-t  
14.40.aq

---

<sup>1</sup> also: IKP (Theorie), Forschungszentrum Jülich, D-52425 Jülich, F.R.G.

<sup>2</sup> also: ITKP, Universität Bonn, D-53115 Bonn, F.R.G.

# 1 Introduction

It is anticipated that future experiments at the Brookhaven Relativistic Heavy Ion Collider (RHIC) will create a highly excited, but nearly baryon-free central zone. At later stages of the collision this zone will contain a dense meson gas, primarily consisting of pions with temperatures of the order of the pion mass. The equation of state and the transport properties of the pion gas are therefore of great current interest [1, 2]. One expects that the  $\pi\pi$  interaction will be modified due to statistical correlations (Bose occupation factors) as well as dynamical (selfenergy) effects [3, 4, 5, 6, 7]. In this context we have previously presented a Brueckner-type calculation for a thermal pion gas treating both effects selfconsistently [8]. To facilitate the numerical calculations we have employed the quasiparticle approximation (QPA) for the single-pion propagator. We have noticed, however, that this approximation becomes unreliable for temperatures above  $T \approx 150$  MeV, *i.e.* in the vicinity of  $T_c$ , the chiral restoration temperature. In addition, recent studies of pion correlations in cold nuclear matter [9] have shown that, for a thorough description of the subthreshold region, it is mandatory to work with a  $\pi\pi$  model which obeys constraints imposed by chiral symmetry. Since chiral symmetry predicts properties of the  $\pi\pi$  interaction in the soft pion limit ( $m_\pi \rightarrow 0$ ), there is an intimate relation between the proper off-shell treatment of in-medium properties and the implementation of chiral constraints.

The aim of the present paper is twofold: first we investigate effects of proper off-shell calculations by comparing them to the QPA results of ref. [8]. This will be discussed in sect. 2. To incorporate constraints from chiral symmetry we then present in sect. 3 an improved version of the  $\pi\pi$  interaction of Lohse et al. [10, 11] which is subsequently used for the in-medium calculations. A short summary and concluding remarks are given in sect. 4.

## 2 Formalism and Results from the Jülich $\pi\pi$ Model

In the  $\pi\pi$  meson exchange model of Lohse et al. [10, 11] the vacuum  $\pi\pi$  T-matrix in a given partial-wave/isospin channel,  $JI$ , is obtained from a Lippmann-Schwinger equation, where the Blankenbecler Sugar reduction scheme [12] of the 4-dimensional Bethe Salpeter equation is adopted:

$$T_{\pi\pi}^{JI}(E, q_1, q_2) = V_{\pi\pi}^{JI}(E, q_1, q_2) + \int_0^\infty dk k^2 4\omega_k^2 V_{\pi\pi}^{JI}(E, q_1, k) G_{\pi\pi}(E, k) T_{\pi\pi}^{JI}(E, k, q_2). \quad (1)$$

Here  $E$  denotes the starting energy of the pion pair and  $q_1, q_2$  are the relative CMS 3-momenta of one pion in the in- and outgoing state, respectively. The interaction kernel  $V_{\pi\pi}^{JI}$  is calculated from an effective meson Lagrangian including  $\rho$ -,  $f_0(1400)$ - and  $f_2(1270)$ -s-channel exchanges, a  $\rho$ -meson exchange in the t-channel as well as coupling to the  $K\bar{K}$  channel (not written explicitly in eq. (1)). The vacuum BbS two-pion propagator in the CMS reads

$$G_{\pi\pi}^0(E, k) = \int \frac{i dk_0}{2\pi} D_\pi(k_0, k) D_\pi(E - k_0, k) = \frac{1}{\omega_k} \frac{1}{E^2 - 4\omega_k^2 + i\eta}, \quad (2)$$

where  $D_\pi(k_0, k)$  denotes the single-pion propagator and  $\omega_k = m_\pi^2 + k^2$ .

At moderate gas densities it is sufficient to treat medium modifications at the one- and two-body level rendering a Brueckner-type description. Leaving the pseudopotentials  $V_{\pi\pi}^{JI}$  temperature independent, which should be a good approximation for temperatures well below the masses of the exchanged mesons, the temperature dependence of the T-matrix is solely induced by the thermal two-pion propagator,  $G_{\pi\pi}^T$ . In terms of the thermal single-pion propagator,  $D_\pi$ , it can be evaluated by means of a Matsubara sum [13, 14]:

$$G_{\pi\pi}^T(\Omega_\lambda, \vec{k}_1, \vec{k}_2) = T \sum_{z_\nu} D_\pi(z_\nu, \vec{k}_1) D_\pi(\Omega_\lambda - z_\nu, \vec{k}_2), \quad (3)$$

with discrete frequencies

$$z_\nu = i\omega_\nu, \quad \Omega_\lambda = i\omega_\lambda, \quad \omega_\nu = 2\pi\nu T, \quad \nu, \lambda \text{ integer}. \quad (4)$$

Using standard techniques of analytical continuation one then obtains

$$G_{\pi\pi}^T(E_+, \vec{k}_1, \vec{k}_2) = \frac{1}{2} \int \frac{d\omega}{\pi} \frac{d\omega'}{\pi} \text{Im}D_\pi(\omega_+, \vec{k}_1) \text{Im}D_\pi(\omega'_+, \vec{k}_2) (1 + f^\pi(\omega) + f^\pi(\omega')) \times \left[ \frac{1}{\omega + \omega' - E_-} + \frac{1}{\omega + \omega' + E_+} \right] \quad (5)$$

where  $\omega_\pm = \omega \pm i\eta$  etc. and  $f^\pi(\omega) = (\exp[\omega/T] - 1)^{-1}$ . For the T-matrix evaluation it will be sufficient to consider  $G_{\pi\pi}^T$  for  $E > 0$  and in the two-pion CMS, *i.e.* in back-to-back kinematics with  $\vec{k}_2 = -\vec{k}_1$ . In this case the imaginary part of eq. (5) receives 2 contributions:

$$\begin{aligned} \text{Im}G_{\pi\pi}^{T,A}(E_+, k) &= - \int_0^E \frac{d\omega}{\pi} [1 + f^\pi(\omega) + f^\pi(E - \omega)] \text{Im}D_\pi(\omega_+, k) \text{Im}D_\pi(E - \omega_-, k), \\ \text{Im}G_{\pi\pi}^{T,B}(E_+, k) &= - \int_E^\infty \frac{2d\omega}{\pi} [f^\pi(\omega - E) - f^\pi(\omega)] \text{Im}D_\pi(\omega_+, k) \text{Im}D_\pi(\omega_+ - E, k) . \end{aligned} \quad (6)$$

In the zero-temperature limit contribution A reproduces the imaginary part of eq. (2), whereas B vanishes. The latter arises solely from thermal excitations. The real part of  $G_{\pi\pi}^T$  is calculated via a dispersion integral [9]:

$$\text{Re}G_{\pi\pi}^T(E, k) = -\mathcal{P} \int_0^\infty \frac{dE'^2}{\pi} \frac{\text{Im}G_{\pi\pi}^T(E'_+, k)}{E^2 - E'^2} . \quad (7)$$

In a second step we evaluate the pion selfenergy,  $\Sigma_\pi$ , which enters the single-pion propagator

$$D_\pi(\omega_+, k) = \frac{1}{(\omega_+)^2 - m_\pi^2 - k^2 - \Sigma_\pi(\omega_+, k)} . \quad (8)$$

At the two-body level  $\Sigma_\pi$  is expressed in terms of the  $\pi\pi$  invariant forward scattering amplitude as

$$\Sigma_\pi(z_\nu, \vec{k}) = - \int \frac{d^3p}{(2\pi)^3} T \sum_{z_{\nu'}} M_{\pi\pi}(z_\nu + z_{\nu'}, \vec{k}, \vec{p}) D_\pi(z_{\nu'}, \vec{p}) , \quad (9)$$

which involves a Matsubara sum over  $z_{\nu'}$ . Using the spectral representations of  $M_{\pi\pi}$  and  $D_\pi$  one arrives at [15]

$$\Sigma_\pi(\omega_+, \vec{k}) = \int \frac{d^3p}{(2\pi)^3} \frac{dE'}{\pi} \frac{d\omega'}{\pi} \text{Im}M_{\pi\pi}(E'_+, \vec{k}, \vec{p}) \text{Im}D_\pi(\omega'_+, \vec{p}) \frac{f^\pi(\omega') - f^\pi(E')}{\omega_+ + \omega' - E'} . \quad (10)$$

The imaginary part of  $\Sigma_\pi$  is given by the  $\delta$ -function contribution of  $1/(\omega_+ + \omega' - E')$ . The positive-energy part of the  $\omega'$  integration gives rise to the standard contribution commonly used in the literature:

$$Im\Sigma_\pi^A(\omega_+, k) = - \int \frac{d^3p}{(2\pi)^3} \int_0^\infty \frac{d\omega'}{\pi} ImM_{\pi\pi}(\omega_+ + \omega', \vec{k}, \vec{p}) ImD_\pi(\omega'_+, \vec{p}) [f^\pi(\omega') - f^\pi(\omega + \omega')] . \quad (11)$$

Note that the Matsubara formalism yields the 'correction'  $f^\pi(\omega + \omega')$  in the occupation factor as was found by Chanfray et al. [7] in the real-time formalism. The negative-energy part of the  $\omega'$  integration can be rewritten by exploiting the symmetry properties of the 1-pion propagator, the  $M_{\pi\pi}$ -amplitude and the Bosefactor resulting in

$$Im\Sigma_\pi^B(\omega_+, k) = - \int \frac{d^3p}{(2\pi)^3} \int_0^\infty \frac{d\omega'}{\pi} ImM_{\pi\pi}(|\omega - \omega'|_+, \vec{k}, \vec{p}) ImD_\pi(\omega'_+, \vec{p}) [\text{sgn}(\omega - \omega') f^\pi(\omega') - f^\pi(|\omega - \omega'|)] . \quad (12)$$

with  $\text{sgn}(\omega - \omega') = \pm 1$ . In analogy to the thermal two-pion propagator (eq. (6)) the contribution B accounts for thermal excitations of the system. E.g. in lowest order,  $Im\Sigma_\pi^B$  is only non-vanishing for  $\omega > 3m_\pi$ . The  $M_{\pi\pi}$ -amplitude is related to the  $T_{\pi\pi}$ -matrix after transforming it into the CMS and identifying the starting energy as  $E^2 \equiv s = (\omega \pm \omega')^2 - (\vec{p} + \vec{k})^2$ :

$$M_{\pi\pi}(\omega \pm \omega', \vec{k}, \vec{p}) = M_{\pi\pi}(\sqrt{s}, q, q) = (2\pi)^3 4\omega_q^2 T_{\pi\pi}(E, q, q) \quad (13)$$

with  $q = q(\omega, \omega', k, p, \cos \Theta)$  being the CMS momentum of both in- and outgoing pions. After a variable transformation  $\cos \Theta \rightarrow E$ , where  $\Theta = \angle(\vec{k}, \vec{p})$ , the final expressions read

$$\begin{aligned} Im\Sigma_\pi(\omega_+, k) &= Im\Sigma_\pi^A(\omega_+, k) + Im\Sigma_\pi^B(\omega_+, k) \\ Im\Sigma_\pi^A(\omega_+, k) &= -\frac{1}{k} \int_0^\infty \frac{p dp}{(2\pi)^2} \int_0^\infty \frac{d\omega'}{\pi} ImD_\pi(\omega'_+, p) [f^\pi(\omega') - f^\pi(\omega + \omega')] I^A \\ Im\Sigma_\pi^B(\omega_+, k) &= -\frac{1}{k} \int_0^\infty \frac{p dp}{(2\pi)^2} \int_0^\infty \frac{d\omega'}{\pi} ImD_\pi(\omega'_+, p) [\text{sgn}(\omega - \omega') f^\pi(\omega') + f^\pi(|\omega - \omega'|)] I^B \end{aligned} \quad (14)$$

with

$$I^{A/B} = \int_{E_{min}^{A/B}}^{E_{max}^{A/B}} dE E M_{\pi\pi}(E, q, q) , \quad (15)$$

where the upper and lower bounds,

$$\begin{aligned} E_{max/min}^A &= (\omega + \omega')^2 - k^2 - p^2 \pm 2kp , \\ E_{max/min}^B &= (\omega - \omega')^2 - k^2 - p^2 \pm 2kp , \end{aligned} \quad (16)$$

correspond to  $\cos \Theta = \mp 1$ , respectively. For the numerical evaluation of  $ImM_{\pi\pi}$  we include all partial waves up to  $J = 2$  and all isospins. Eq. (10) evades a 'direct' calculation of  $Re\Sigma_{\pi}(\omega, k)$  in terms of  $ReM_{\pi\pi}$  due to the  $E'$ -dependence of the occupation factor. Therefore we again make use of a dispersion relation including a subtraction at  $\omega = 0$ :

$$Re\Sigma_{\pi}(\omega, k) = -\mathcal{P} \int_0^{\infty} \frac{d\omega'^2}{\pi} \frac{Im\Sigma_{\pi}(\omega'_+, k)}{\omega^2 - \omega'^2} \frac{\omega^2}{\omega'^2} . \quad (17)$$

The subtraction is dictated by the fact that  $Re\Sigma_{\pi}(\omega, k) \rightarrow 0$  for  $\omega \rightarrow 0$ . To check the subtraction procedure numerically we have performed calculations by approximating  $f^{\pi}(E') \approx f^{\pi}(\omega + \omega')$  in eq. (10), which allows to reinsert the spectral representation of  $M_{\pi\pi}$ .  $Re\Sigma_{\pi}$  can then be calculated directly in terms of  $ReM_{\pi\pi}$  (in exact analogy to calculating  $Im\Sigma_{\pi}$  in terms of  $ImM_{\pi\pi}$ ). The results of this test calculation coincide within a few percent with the results obtained from eq. (17). Eqs. (1), (6)-(8) and (14), (17) form the selfconsistent set of equations which is solved by numerical iteration.

The results for the imaginary part of the  $\pi\pi$  M-amplitude are displayed in Fig. 1. With increasing temperature we find in the  $\sigma$ -channel ( $JI=00$ ) a considerable enhancement over the vacuum curve for CMS energies below  $E \approx 450$  MeV. Apart from the highest temperature ( $T=200$  MeV) there is, however, no significant strength below  $2m_{\pi}$ . For  $T=200$  MeV some accumulation of subthreshold strength is found which is almost entirely due to thermal excitations (the 'B'-contribution in eq. (6)). For comparison, results within the QPA are also given (in contrast to ref. [8] the 'polestrength'  $z_k = (1 - \partial Re\Sigma_{\pi}(\omega, k)/\partial\omega^2|_{e_k})^{-1}$  is not included since it leads to a violation of the normalization condition of the 1-pion

spectral function). For the  $\rho$ -channel ( $JI=11$ ) both the full and the QPA results show a broadening of the resonance, increasing with temperature due to the thermal motion of the gas particles. The QPA results clearly overestimate the thermal broadening and the upward peakshift of the  $\rho$  resonance.

A comment concerning the QPA calculations of refs. [8, 16] is in order. When expanding around the quasiparticle pole, in next-to-leading order a complex polestrength  $z_k$  arises. This results in a strong enhancement of  $ImM_{\pi\pi}$  in the vicinity of resonance peaks. Such a strong enhancement is not confirmed by the full calculations presented here. At intermediate energies the full calculations do show an enhancement over the QPA results, however.

### 3 $\pi\pi$ Interaction with Chiral Constraints

For the subthreshold  $\pi\pi$  amplitude in cold nuclear matter the implementation of properties dictated by chiral symmetry has turned out to be crucial [9]. To see the impact of such constraints on the interacting pion gas we have improved the Jülich model employed in the previous section in two respects (for a detailed discussion see refs. [17, 9]):

- we introduce  $\pi\pi$  contact interactions as obtained from the gauged nonlinear  $\sigma$  model of Weinberg [18]. At the tree level these contributions ensure the correct values of the  $\pi\pi$  amplitude at both the soft point and the Adler point. When supplemented with phenomenological form factors,  $F(q) = (2\Lambda^2 - 4m_\pi^2)^2 / (2\Lambda^2 + 4q^2)^2$ , they are suitable for iteration in the T-matrix equation (1);
- instead of using the on-energy-shell prescription implied by the BbS formalism we here employ an on-mass-shell prescription for the off-shell values of the pseudopotentials  $V_{\pi\pi}^{JI}$ . In this way we are able to impose the correct chiral limit of the s-wave scattering lengths, *i.e.*  $a^{0I} \rightarrow 0$  for  $m_\pi \rightarrow 0$  (the model of Lohse et al. [10] does not have this property).

With similar cutoff parameters as in [10] the results of refitting the vacuum  $\pi\pi$  scattering data are quite satisfactory (see Fig. 2). The additional cutoff parameters in the contact terms are chosen to be slightly below 1 GeV. For the s-wave scattering lengths we obtain  $a^{00} = 0.21m_\pi^{-1}$ ,  $a^{02} = -0.028m_\pi^{-1}$ , in reasonable agreement with a recent experimental analysis [19].

With this 'chirally improved' model we have repeated the selfconsistent in-medium calculations described in the previous section. The results are displayed in Fig. 3. We again observe a reduction of the peak values in both  $\sigma$ - and  $\rho$ - channel of the  $\pi\pi$  scattering amplitude. The effects are smaller than in the original Jülich model. There remains some enhancement over the vacuum curve in the low-energy region and there is very little strength below threshold. This can be attributed to the subthreshold repulsion induced by the contact interactions.

## 4 Summary

Within the finite temperature Green's function method [13, 15] we have derived expressions for the pion selfenergy and the uncorrelated  $2\pi$  propagator in a hot pion gas in thermal as well as chemical equilibrium ( $\mu_\pi = 0$ ). Starting from the vacuum  $\pi\pi$  model of Lohse et al. [10] these have been used to calculate medium modifications at the one- and two-body level *selfconsistently*, *i.e.* the in-medium scattering amplitude was evaluated in terms of the pion selfenergy and vice versa. It has been shown that the full off-shell calculations differ from the QPA in the following respects: in the intermediate-energy range ( $E \approx 300$ -800 MeV) the imaginary part of the  $\pi\pi$  amplitude shows less suppression compared to the vacuum curve; thermal excitation contributions (not present in the QPA) lead to some subthreshold strength in the  $\sigma$  channel at temperatures around 200 MeV; in particular, the QPA calculations overestimate the thermal broadening and the upward peakshift of the  $\rho$  resonance.

Motivated by a recent analysis of  $\pi\pi$  correlations in cold nuclear matter [9], we have also



studied a 'chirally improved' version of the Jülich  $\pi\pi$  model. Applying this model to the hot pion gas it is found that the subthreshold strength almost entirely disappears due to the additional repulsion induced by the chiral constraints. Also the enhancement just above the two-pion threshold is much less pronounced. The in-medium features of the  $\pi\pi$  amplitude for higher energies (reduction of the peak values in both  $\sigma$  and  $\rho$  channel, essentially no peakshift of the  $\rho$  resonance) are in good agreement for both models. After all, the deviations from the  $\pi\pi$  interaction in free space are rather small.

In conclusion, we wish to stress that proper off-shell calculations beyond the QPA and the inclusion of constraints from chiral symmetry are necessary to obtain reliable results for the pion selfenergy and the in-medium  $\pi\pi$  amplitudes of a hot pion gas. The latter could serve as an input for transport models simulating the time evolution of ultrarelativistic heavy-ion collisions [20] near freeze-out.

### Acknowledgement

We thank G.G. Bunatian, G. Chanfray, J. Durso, B. Friman and J. Speth for useful discussions. One of us (R.R.) acknowledges financial support by Deutscher Akademischer Austauschdienst (DAAD). This work was supported in part by a grant from the National Science Foundation, NSF-PHY-89-21025.

## References

- [1] G.G. Bunatian and B. Kämpfer, preprint FZR 93-28.
- [2] S. Gavin, Nucl. Phys. **B351** (1991) 561.
- [3] E.V. Shuryak, Nucl. Phys. **A533** (1991) 761.
- [4] Z. Aouissat, G. Chanfray, P. Schuck and G. Welke, Zeit. Phys. **A340** (1991) 347.
- [5] A. Schenk, Nucl. Phys. **B363** (1991) 97.
- [6] H.W. Barz, G.F. Bertsch, P. Danielewicz and H. Schulz, Phys. Lett. **B275** (1992) 19.
- [7] G. Chanfray and D. Davesne, to be published.
- [8] R. Rapp and J. Wambach, Phys. Lett **B315** (1993) 220.
- [9] Z. Aouissat, R. Rapp, G. Chanfray, P. Schuck and J. Wambach, Nucl. Phys. **A581** (1995) 471.
- [10] D. Lohse, J.W. Durso, K. Holinde and J. Speth, Phys. Lett. **B234** (1989) 235; Nucl. Phys. **A516** (1990) 513.
- [11] B. C. Pearce, K. Holinde and J. Speth, Nucl. Phys. **A541** (1992) 663.
- [12] R. Blankenbecler and R. Sugar, Phys. Rev. **142** (1966) 1051.
- [13] L.P. Kadanoff and G.A. Baym, 'Quantum Statistical Mechanics', Benjamin, New York 1962.
- [14] L.D. Fetter and J.D. Walecka, 'Quantum Theory of Many Particle Systems', Mc Graw Hill, New York 1971.
- [15] M. Schmidt, G. Röpke and H. Schulz, Ann. Phys. **202** (1990) 57.

- [16] R. Rapp and J. Wambach, Nucl. Phys. **A573** (1994) 626.
- [17] J. Durso, R. Rapp and J. Wambach, to be published.
- [18] S. Weinberg, Phys. Rev. Lett. **17** (1966) 616
- [19] H. Burkhardt and J. Lowe, Phys. Rev. Lett. **67** (1991) 2622.
- [20] G.M. Welke and G.F. Bertsch, Phys. Rev. **C45** (1992) 1403; H.W. Barz, P. Danielewicz, H. Schulz and G.M. Welke, Phys. Lett. **B287** (1992) 40.

## FIGURE CAPTIONS

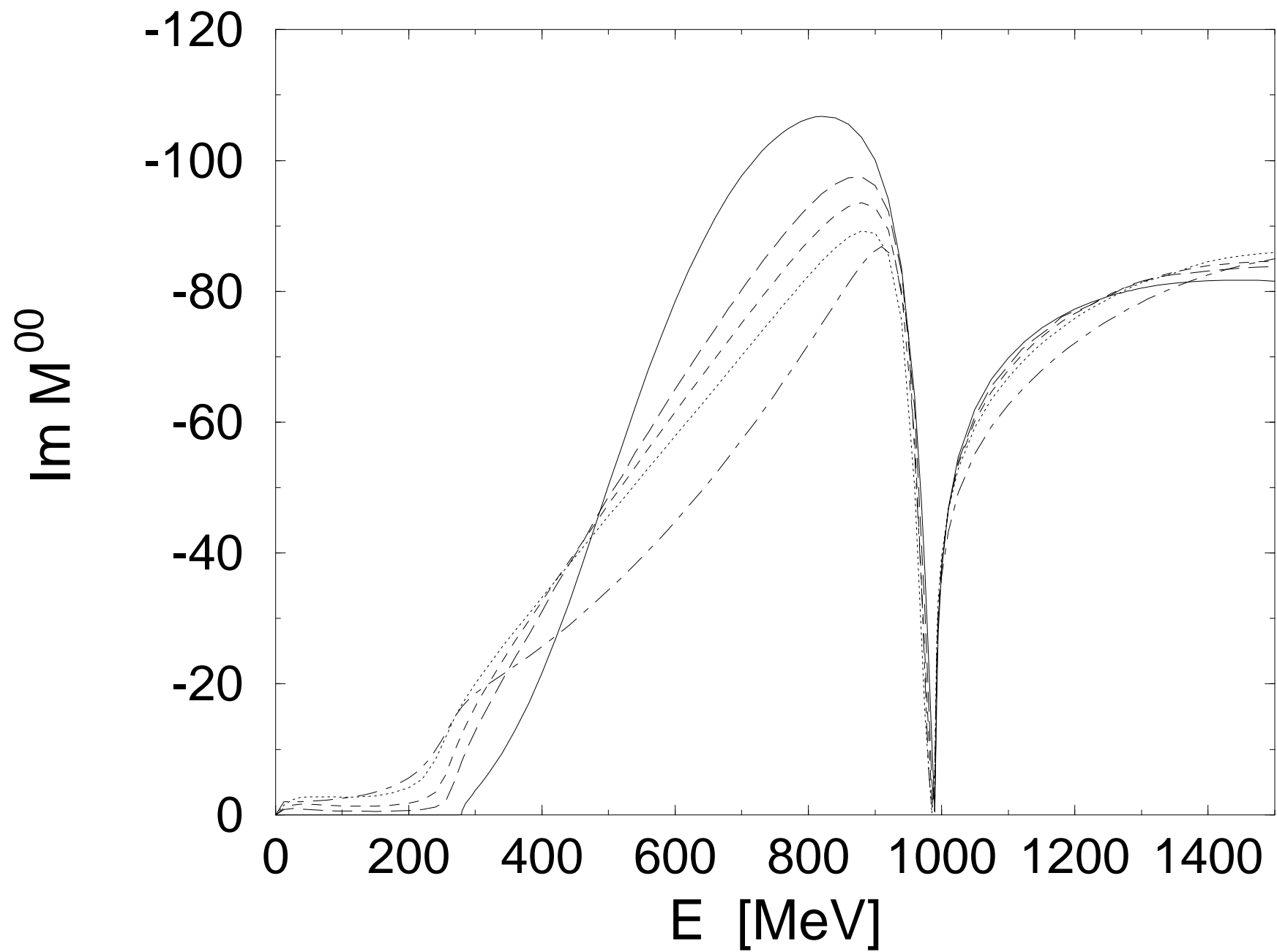
**Fig. 1:** The imaginary part of the  $\pi\pi$  M-amplitude in  $\sigma$  ( $JI=00$ ) and  $\rho$  ( $JI=11$ ) channel in a hot pion gas at  $\mu_\pi=0$ . The long-dashed, short-dashed and dotted lines are the selfconsistent results of the full off-shell calculations at temperatures  $T=150,175$  and  $200$  MeV, respectively. The dashed-dotted line represents the selfconsistent QPA calculation at  $T=200$  MeV. The full line corresponds to the vacuum amplitude within the non-chirally symmetric Jülich model.

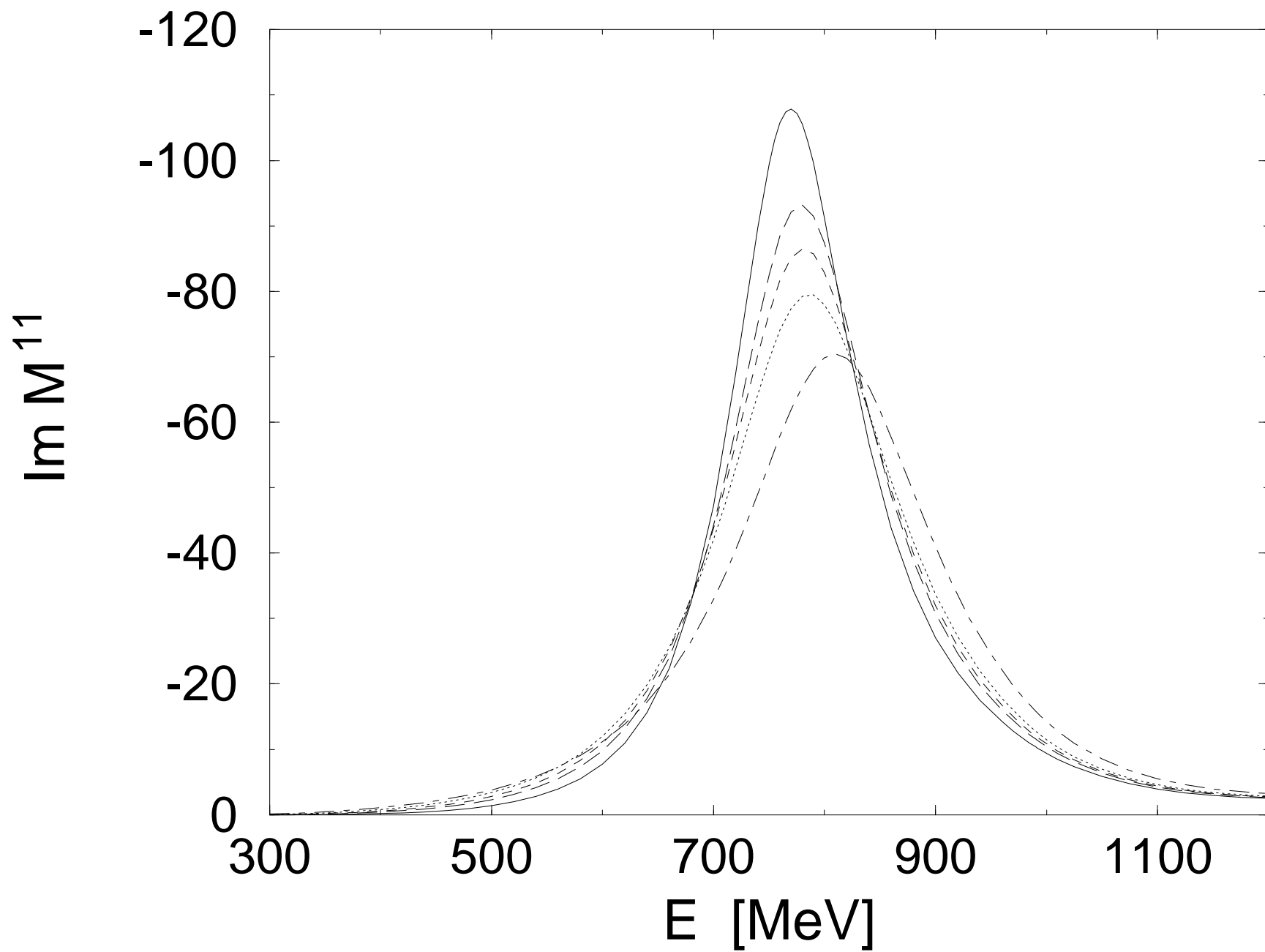
**Fig. 2:** A fit to the vacuum  $\pi\pi$  scattering phase shift data obtained within the chirally improved Jülich model.

**Fig. 3:** The imaginary part of the  $\pi\pi$  M-amplitude in  $\sigma$  and  $\rho$  channel in a hot pion gas at  $\mu_\pi=0$ . All curves are calculated by means of the chirally improved Jülich model (full line: free space; temperature identification as in fig. 1). The in-medium results are from selfconsistent, full off-shell calculations as described in sect. 2.

This figure "fig1-1.png" is available in "png" format from:

<http://arxiv.org/ps/nucl-th/9502023v2>

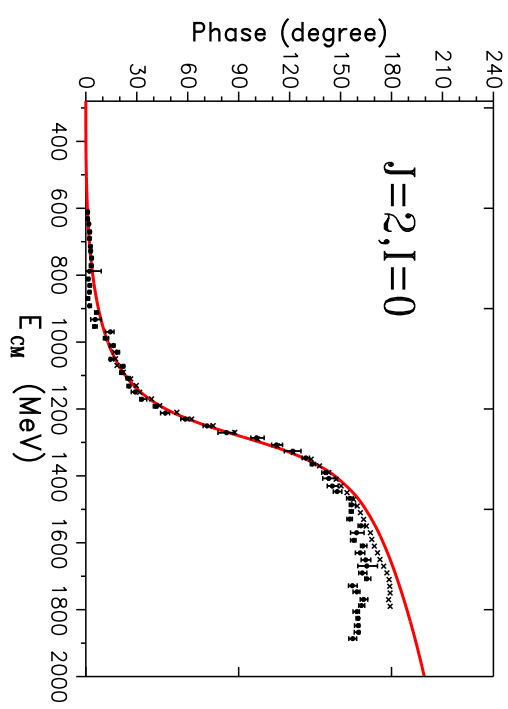
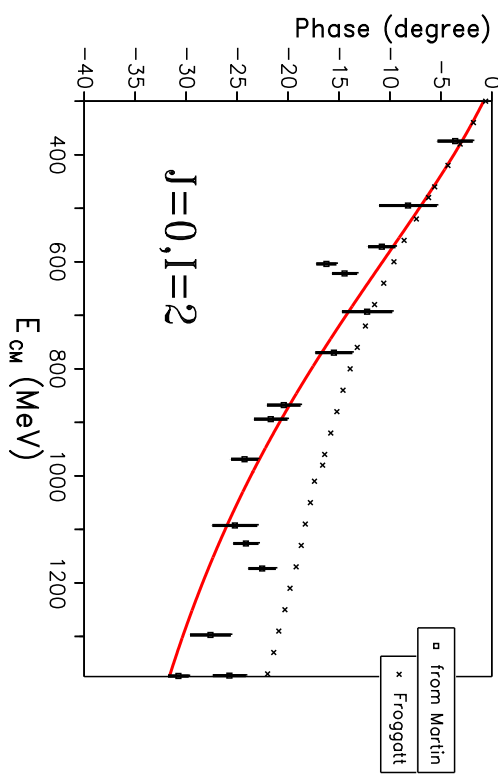
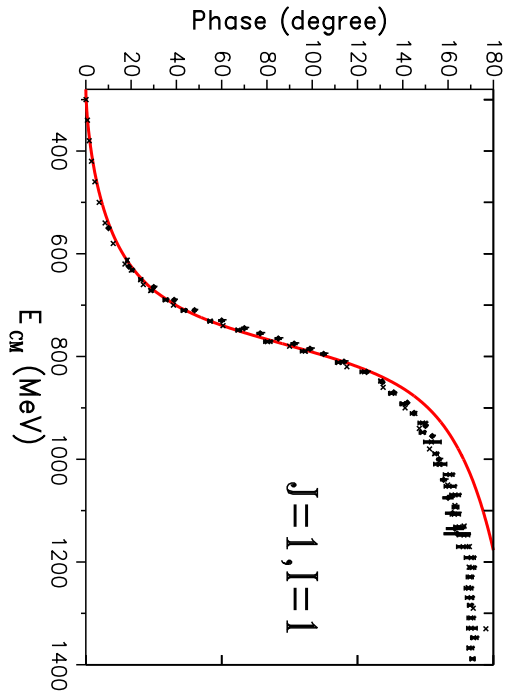
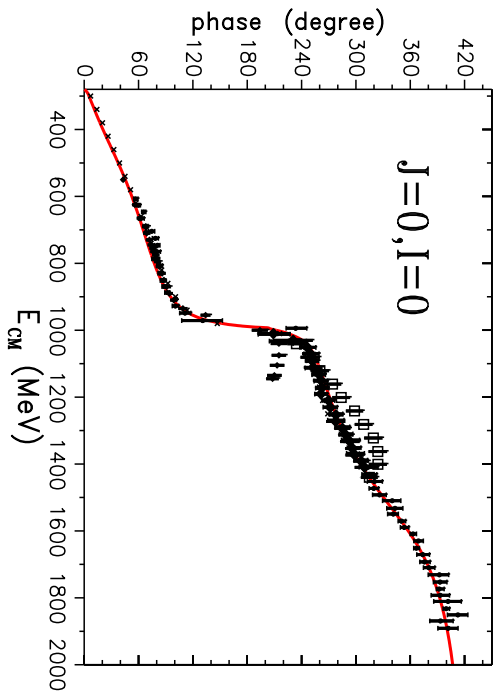




This figure "fig1-2.png" is available in "png" format from:

<http://arxiv.org/ps/nucl-th/9502023v2>





This figure "fig1-3.png" is available in "png" format from:

<http://arxiv.org/ps/nucl-th/9502023v2>

